Ring-opening polymerization of six-membered cyclic hybrid dimers composed of an oxoester and thioester

Mao Hirata[1] · Tomoki Yoshimatsu[1] · Shin-ichi Matsuoka ⓘ[1] · Susumu Kawauchi[2,3] · Masato Suzuki[1]

Abstract

Three cyclic oxoester-thioester hybrid monomers, **1** (3-methyl-1,4-oxathiane-2,5-dione), **2** (6-methyl-1,4-oxathiane-2,5-dione), and **3** (3,6-dimethyl-1,4-oxathiane-2,5-dione), were studied for anionic and cationic ring-opening polymerizations. These monomers are six-membered cyclic cross-dimers corresponding to combinations of glycolic and lactic acids with their thiol analogs. Anionic polymerizations using thiol as the initiator and 2,6-lutidine as the base catalyst were successful for the chemoselective cleavage of the thioester with the thiol propagating end. The polymerizability increased in the order of **3 < 1 < 2**, which was in good agreement with the increasing ring strain order evaluated by Density Functional Theory calculations. The living character, to some extent, was suggested by the postpolymerization reactions, which involved a two-stage feed of the monomers and a thiol-ene terminal coupling reaction to form a block copolymer with PEG. Additionally, it was found that the polymerization took place in 2,6-lutidine without a thiol initiator and produced macrocyclic polymers. The cationic polymerizations took place with the aid of CF_3SO_3H and benzyl alcohol but involved side reactions with low chemoselective ring cleavage. The thioester unit caused the polymers to exhibit a lower T_g with greater thermal and photo degradability.

Introduction

Compared with the usual carboxylic ester, thioester has a more electrophilic carbonyl carbon (Character 1) and forms a more stable carbonyl α-anion (Character 2) due to the weaker π-n conjugation between the carbonyl group and the sulfur atom. These characteristics play essential roles in the bioreaction of trans-acylation and C-C bond formation, representatively, through metabolic pathways related to CoA. However, thioesters have rarely been studied for polymer synthesis, while there are a huge number of studies on polyesters and polyamides.

We have engaged in the elucidation of thioester chemistry in the field of polymerization. Characters 1 and 2 of thioester prompted two research projects, i.e., ring-opening polymerization (ROP) of thiolactone and anionic polymerization of (meth)acrylic thioester, respectively. We have already reported that highly strained β-thiolactone undergoes thiol-initiated ROP without the use of a catalyst [1]. Less-strained *rac*-thiolactide was found to require amine catalysts for equilibrium polymerization [2]. It has been revealed that an acrylic thioester undergoes anionic polymerization via a twitter ionic mechanism initiated by amines, demonstrating higher anionic polymerizability than that of acrylate [3].

Recently, related studies based on Character 1 have increased in number. They include not only studies on ROPs but also those focusing on polycondensation, polyaddition, polymer reactions at the side and main chains, and ligations at the polymer terminal groups [4–12]. Trends in sustainable chemistry prompted the study of reversible ROPs by using the dynamic property of thiol-thioester exchange reactions [7, 9–12]. Tao et al. reported that six-

✉ Masato Suzuki
   m.suzuki.358@nitech.jp

[1] Department of Life Science and Applied Chemistry, Nagoya Institute of Technology, Nagoya 466-8555, Japan

[2] Laboratory for Materials and Structures, Institute for Innovative Research, Tokyo Institute of Technology, 2-12-1 Ookayama, Meguro-ku, Tokyo 152-8550, Japan

[3] Quemix Inc., 16F, Taiyo Life Nihonbashi Bldg, 2-11-2 Nihonbashi, Chuo-ku, Tokyo 103-0027, Japan

membered dithiolactones, including thiolactide, are monomers that perform well [11]. His group very recently extended a similar work for monothiodilactones consisting of a glycolic thioester component [12]. Independently, we have also extended our previous studies mentioned above for the ROP of six-membered cyclic hybrid dimers composed of an oxoester and thioester (monomers **1, 2**, and **3**, Scheme 1) since 2019. We undertook this project to examine the selective ring cleavage of the thioester and oxoester parts. The anionic condition is expected to result in thioester cleavage due to its higher electrophilicity. Monomer **1** has been employed also by Tao et al. and revealed to undergo such ROP [12]. On the other hand, it is possible that the oxoester is more reactive under acidic conditions, which was investigated in this article. How the methyl substituent on the monomer ring affects the ROP has also been investigated. The chemo- and regioselective ROPs are known for other six-membered cyclic hybrid dimers consisting of amide-oxoester, amide-thioester, and glycolic-lactic oxoesters [13, 14]. Therein, ROPs are generated at the oxoester and thioester due to the much lower reactivity of the amide group [13], and methylglycolide undergoes ROP via lactyl cleavage [14]. These works produce polymers consisting of alternating units; amide-oxoester, amide-thioester, and glycolic-lactic oxoester polymers are obtained in a controlled fashion. The hybrid monomers studied herein are expected to yield polymers composed of alternating oxoester-thioester units.

Experimental section

General methods and materials

The instruments, measurement conditions, and material information are described in the Supplementary Information.

Synthesis of monomer 1 (3-methyl-1,4-oxathiane-2,5-dione)

Thiolactic acid (8.7 mL, 0.1 mol) was slowly added via a syringe to bromoacetyl bromide (8.8 mL, 0.1 mol) in a two-neck flask under N_2. The mixture was stirred at r.t. overnight, while the evolved HBr gas was introduced over NaOH aq. through an outlet natural rubber tube with an N_2 stream. Water (200 mL) was added to the reaction mixture, which was subsequently extracted with CH_2Cl_2 (2×200 mL). The combined organic layer was washed with brine, dried over $MgSO_4$, and concentrated in vacuo. The product was used for cyclization without further purification.

The residue (16.46 g, 72.4 mmol) was dissolved in dry MeCN (200 mL) under N_2 and cooled to 0 °C. Dry $(^iPr)_2NEt$ (12 mL, 70.6 mmol) dissolved in dry MeCN (17 mL) was added via a syringe. The mixture was then allowed to warm to room temperature and stirred overnight. Diethyl ether was added, and $(^iPr)_2NEt$ hydrobromide was removed by filtration. The filtrate was evaporated under reduced pressure, and the crude mixture was purified by silica gel column chromatography (CH_2Cl_2, $R_f = 0.47$). The product was distilled (131 °C/270 Pa), yielding **1** as a colorless liquid (2.16 g, 20% yield), which was crystallized in a refrigerator (m.p. 41.4–42.5 °C). ^1H NMR (CDCl$_3$, Fig. S1): δ 1.62 (d, $J = 6.9$ Hz, 3H), 4.21 (q, $J = 6.9$ Hz, 1H), 4.75 (d, $J = 15.3$ Hz, 1H), 4.93 (d, $J = 15.3$ Hz, 1H). ^{13}C NMR (CDCl$_3$, Fig. S2): δ 14.45, 36.00, 74.07, 168.20, 194.88. IR (KBr): Fig. S3. MS (EI, m/z): Found 146.0027, Calc. 146.0038 (M$^+$).

Synthesis of monomer 2 (6-methyl-1,4-oxathiane-2,5-dione)

Monomer **2** was prepared by the same procedure as **1**. Starting from thioglycolic acid (6.14 mL, 0.093 mol) and 2-bromopropionyl bromide (9.75 mL, 0.093 mol), **2** was produced via the crude precursor (17.6 g, 77.5 mmol). Monomer **2** was purified by silica gel column chromatography (CH_2Cl_2, $R_f = 0.41$) and subsequent vapor-diffusion recrystallization (EtOAc with CCl_4) in 37% yield (4.14 g, m.p. 101.3–102.4 °C). ^1H NMR (CDCl$_3$, Fig. S4): δ 1.58 (d, $J = 6.5$ Hz, 3H), 3.70 (d, $J = 15.2$ Hz, 1H), 4.13 (d, $J = 15.2$ Hz, 1H), 4.98 (q, $J = 6.5$ Hz, 1H). ^{13}C NMR (CDCl$_3$, Fig. S5): δ 14.91, 30.06, 79.84, 165.29, 196.13. IR (KBr): Fig. S6. MS (EI, m/z): Found 146.0039, Calc. 146.0038 (M$^+$).

Synthesis of monomer 3 (3,6-dimethyl-1,4-oxathiane-2,5-dione)

Monomer **3** was prepared by the same procedure as **1**. Starting from thiolactic acid (4.42 mL, 0.05 mol) and 2-bromopropionyl bromide (5.27 mL, 0.093 mol), **3** was produced via the crude precursor (8.77 g, 36.4 mmol). Monomer **3** was purified twice by silica gel column chromatography (hexane/EtOAc = 5/3, $R_f = 0.46$, and subsequently CH_2Cl_2, $R_f = 0.55$) in 42% yield (2.44 g, *RR* and *SS* isomers/*RS* and *SR* isomers = 95/5, m.p. 34.3–35.5 °C). ^1H NMR (CDCl$_3$, Fig. S7) of the *RR* and *SS* isomers: δ 1.57 (d, $J = 6.5$ Hz, 3H), 1.60 (d, $J = 6.8$ Hz, 3H), 4.28 (q, $J = 6.8$ Hz, 1H), 5.02 (q, $J = 6.5$ Hz, 1H); the *RS* and *SR* isomers: δ 1.67 (d, $J = 7.1$ Hz, 3H), 1.71 (d, $J = 7.2$ Hz, 3H), 4.19 (q, $J = 7.2$ Hz, 1H), 5.03 (q, $J = 7.1$ Hz, 1H). ^{13}C NMR (CDCl$_3$, Fig. S8) of the *RR* and *SS* isomers: δ 14.18; 14.68; 37.03; 79.90; 168.70; 196.76. IR (KBr): Fig. S9. MS (EI, m/z): Found 160.0219, Calc. 160.0194 (M$^+$).

A representative procedure for anionic polymerization

Monomer **1** (100 mg, 0.684 mmol) was dissolved in dry CH_2Cl_2 (0.46 mL) in a test tube under N_2. A solution of dry

2-ethylhexyl thioglycolate (140 μL, 136 mg, 0.666 mmol) in dry CH_2Cl_2 (2.0 mL, 2.730 g) was prepared in advance, and a portion (147 mg, 0.0342 mmol of 2-ethylhexyl thioglycolate) was added to the test tube. Another solution of dry 2,6-lutidine (163 μL, 150 mg, 1.40 mmol) in dry CH_2Cl_2 (2.0 mL, 2.688 g) was also prepared in advance, and a portion (138 mg, 0.068 mmol of 2,6-lutidine) was subsequently added to the test tube. The mixture was stirred under a closed system at r.t. for 24 h. Amberlyst 15E (15 mg, H^+ = 0.071 mmol) was added to the reaction mixture to exclude 2,6-lutidine. After 30 min of stirring, the supernatant collected by filtration was dried under vacuum and analyzed by ^{1}H NMR spectroscopy and GPC. The polymer was isolated by reprecipitation into diethyl ether. The ^{1}H and ^{13}C NMR and IR spectra of Poly1–3 are available in the Supplementary Information (Figs. S11–S19).

A representative procedure for cationic polymerization

Monomer **1** (100 mg, 0.684 mmol) was dissolved in dry CH_2Cl_2 (0.65 mL) in a test tube under N_2. A solution of dry benzyl alcohol (35.5 μL, 37.0 mg, 0.342 mmol) in dry CH_2Cl_2 (0.3 mL, 0.396 g) was prepared in advance, and a portion (43.6 mg, 0.0342 mmol of benzyl alcohol) was added to the test tube. Subsequently, trifluoromethanesulfonic acid (5.2 mg, 0.034 mmol) was also added. The mixture was stirred under a closed system at r.t. for 24 h. Amberlyst 21 (8 mg, base = 0.034 mmol) was added to the reaction mixture to remove the acid. After 30 min of stirring, the supernatant collected by filtration was dried under vacuum and analyzed by ^{1}H NMR spectroscopy and GPC.

Synthesis of the block copolymer by the thiol-ene coupling reaction

The dried reaction mixture (64.9 mg) of poly**1**, which was prepared in the presence of 2-ethylhexyl thioglycolate (6.93 mol% for monomer **1**, 0.023 mmol) with 2,6-lutidine, was transferred into a Pyrex® test tube. Norbornene-terminated PEG 2000 (73 mg, 0.034 mmol) and DMPA (2,2-dimethoxy-2-phenylacetophenone) (2.9 mg, 0.009 mmol) were added, and then CH_2Cl_2 (0.4 mL) was added under N_2. The solution was degassed by three consecutive freeze–pump–thaw cycles. This mixture was subjected to irradiation from a high-pressure Hg lamp for 4 h. The resultant solution was dried in vacuo and analyzed by GPC.

A typical procedure for UV-photolysis of the polymer

A CH_2Cl_2 (0.3 mL) solution of poly**1** (3 mg, [C(= O) S] = 68.5 mM) in a quartz test tube was exposed to a low-pressure Hg lamp under N_2 at r.t. After 3 h, a small aliquot from the CH_2Cl_2 solution was subjected to GPC analysis.

Calculation methods

The density functional theory (DFT) calculation methods are described in our previous study [2], and the detailed results are available in the Supplementary Information.

Results and discussion

Monomer synthesis

Monomer **1** was prepared from bromoacetyl bromide and thiolactic acid (Scheme 1) by a modified procedure from a previous report [15]. This procedure was also applied in the preparation of monomers **2** and **3**. The ^{1}H NMR spectrum (Fig. S7) suggested that the obtained monomer **3** was a diastereomeric mixture (95/5). The major diastereomers were identified by the NOESY spectrum as the *RR* and *SS* isomers (Fig. S10). A cross peak between the two methine protons of the major diastereomer was observed, suggesting that it has *RR* and *SS* stereochemistry.

Anionic polymerization by combining a thiol initiator with 2,6-lutidine

In a previous report from our group, pyridine was found to effectively catalyze the bulk polymerization of thiolactide [2]. Thus, the ring-opening polymerizations of monomers **1**, **2**, and **3** were investigated by using a combination of 2-ethylhexyl thioglycolate as the initiator with pyridine as the catalyst in CH_2Cl_2 at r.t. (Table 1). However, the polymerizations were so slow in producing the oligomer that the stronger base 2,6-lutidine ($pKa = 6.60$ in H_2O) (https://pubchem.ncbi.nlm.nih.gov/) was employed in place of pyridine ($pKa = 5.23$ in H_2O) (https://pubchem.ncbi.nlm.nih.gov/). As expected, the polymerizations were more efficient for monomers **1** and **2** (Table 2). Increasing the amount of 2,6-lutidine from 5 mol% to 10 mol% apparently accelerated the polymerization. Figure 1 shows the living characteristics of the polymerizations of **1** and **2** at the stages at which the low-molecular-weight polymers were produced. However, decreasing the amount of initiator produced a higher molecular weight polymer, which was not precisely controllable. For example (Entry 9), using 1 mol% initiator afforded a polymer with $Mn = 7100$, which was much smaller than the theoretical value of 11500 (monomer conv. = 79%); this is probably due to the back-biting reaction (vide infra), the relative rate of which increases in comparison with that of propagation at a low concentration of the initiator, causing a larger PDI.
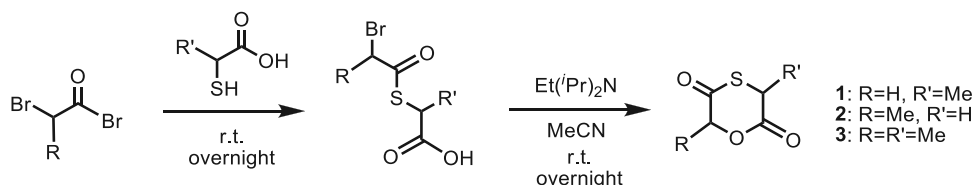
Scheme 1 Monomer syntheses

1: R=H, R'=Me
2: R=Me, R'=H
3: R=R'=Me

Table 1 Anionic polymerization of monomers **1**, **2**, and **3** in CH_2Cl_2 at r.t using 2-ethylhexyl thioglycolate as the initiator and pyridine as the catalyst

Entry	Monomer[a]	Init. (mol%)	Pyridine. (mol%)	Time (day)	Conv.[b] (%)	M_n[c]	PDI[c]
1	**1**	5	5	5	14	690	1.16
2	**2**	5	5	5	23	800	1.32
3	**3**	5	5	5	10	600	1.18

[a][Monomer] = 1 M
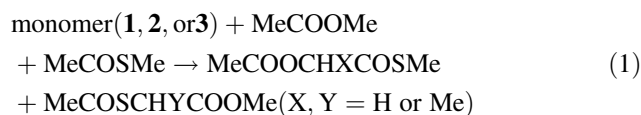
[b]Determined by ^1H NMR spectroscopy

[c]GPC (THF, PSt std.) profile of the reaction mixture

In agreement with our expectation, as suggested by the ^1H NMR spectra of the obtained polymers, ring opening selectively occurs at the C(=O)-S bond and the propagating chain end is the thiol group. Figure 2 shows signals due to the terminal protons, i.e., the methine and thiol, produced from monomer **1**. Their peak assignment was assisted by the spectrum of the stoichiometric reaction mixture of monomer **1** with the initiator (Fig. S20). The signal due to the thiol proton disappeared upon the addition of a drop of D_2O. Similarly, selective ring cleavage at the thioester was also confirmed for monomers **2** and **3** (Figs. S21–S24).

Table 2 suggests that monomers **3**, **1**, and **2** are in order of increasing polymerizability. The time-conversion curves of monomers **1** and **2** also suggested that **2** was more reactive (Fig. 3A). As shown in Fig. 3B, the propagating end of poly**1** is the secondary thiol, which attacks the α-unsubstituted thioester carbonyl. On the other hand, in the propagation of poly**2**, the primary thiol reacts with the α-methyl thioester carbonyl; the experimental results suggest that the latter is faster, which is consistent with the literature about regioselective ring opening in the polymerization of methylglycolide, initiated by alcohol with a base [14]. The propagating end is the primary alcohol, which selectively attacks the α-methyl ester carbonyl. Because of the steric hindrance between the two methyl groups located at the propagating end and at the monomer, the polymerization rate of monomer **3** is the lowest.

Thermodynamic consideration of the ring strain of monomers **1**–**3** provides additional insight into their polymerizability. DFT calculations (ωB97X-D/6-311 + G(d,p) with PCM toluene) [2] were used to evaluate the ring strain

energy by using homodesmotic reactions (Eq. (1)).

$$\text{monomer}(\mathbf{1}, \mathbf{2}, \text{or} \mathbf{3}) + \text{MeCOOMe}$$
$$+ \text{MeCOSMe} \rightarrow \text{MeCOOCHXCOSMe} \qquad (1)$$
$$+ \text{MeCOSCHYCOOMe}(X, Y = H \text{ or } Me)$$

The ring strain energy values (ΔH) are 8.96, 9.82, and 8.47 kcal/mol for monomers **1**, **2**, and **3** (the *RR* and *SS* isomers), respectively. Thus, the thermodynamic aspect also suggests that the order of increasing polymerizability is **3** < **1** < **2**, which is consistent with the experimental results. In a previous study by our group [2], the same DFT calculations for *rac*-thiolactide and *rac*-lactide revealed that their ring strain energies were 5.45 and 11.27 kcal/mol, respectively. Monomer **3** is a hybrid compound and reasonably has a medium ring strain. The longer bond length of the sulfur atom reduces the strain of the six-membered bislactone ring.

Figure 4 shows the MALDI-TOF-MS spectrum of the polymerization mixture of monomer **1** (Entry 2, Table 2). Two types of regular peak series were observed for the polymers. One is due to the linear polymer, whose terminals have an initiator fragment and a thiol proton, and the other is ascribable to the cyclic polymer, which is produced by the backbiting reaction. Poly**2** was also revealed to contain both linear and cyclic structures (Fig. S25). However, their relative contents are not informed by the MS spectra, so chain extension experiments were performed. Either monomer **1** or monomer **2** was added to the polymerization mixture, and the products were analyzed by GPC before and after polymerization (Fig. 5). The GPC profiles clearly shift to the higher molecular weight region, suggesting that chain extension occurred from the thiol terminals of the linear polymers and that the relative contents of the cyclic polymers were very small. Another chain extension experiment involves a thiol-ene reaction to form a block copolymer [1]. The terminal thiol groups of the linear polymers from **1** and **2** were subjected to photoinitiated radical addition to the norbornene group at the PEG (MW2000) terminal (Scheme 2). Compared with those of the starting polymers, the GPC profiles of the reaction mixtures shifted to the higher molecular weight region (Fig. 6 and S26). When 1.5 eq of PEG was added, the RI detector showed a bimodal GPC profile due to the block copolymer with unreacted PEG. On the other hand, the UV detector shows no peak due to the presence of PEG, which absorbs no

Table 2 Anionic polymerization of monomers **1**, **2**, and **3** in CH$_2$Cl$_2$ at r.t using 2-ethylhexyl thioglycolate as the initiator and 2.6-lutidine as the catalyst

Entry	Monomer[a]	Init. (mol%)	Lutidine (mol%)	Time (day)	Conv.[b] (%)	M_n[c]	PDI[c]
1	**1**	6	5	1	28	1050	1.13
				3	51	1900	1.12
2	**1**	6	10	1	71	2700	1.13
3	**1**	5	10	5	87	3100	1.33
4	**1**	2	10	2	51	4600 (4600[d])	1.12 (1.12[d])
5	**2**	6	5	1	71	1800	1.23
				2	84	2400	1.26
6	**2**	6	10	1	83	2900	1.17
7	**2**	5	10	5	96	3400	1.34
8	**2**	2	10	2	66	5900 (6100[d])	1.18 (1.15[d])
9	**2**	1	5	4	79	7100	1.86
10	**3**	5	5	1	15	600	1.20
				3	23	1000	1.23

[a][Monomer] = 1 M

[b]Determined by ^{1}H NMR spectroscopy

[c]GPC (THF, PSt std.)

[d]After reprecipitation into Et$_2$O. (yield=52% (Entry 4), 62% (Entry 8))

Fig. 1 Conversion dependence of M_n and M_w/M_n of polymers from **1** (**a**) and **2** (**b**) in the presence of 2-ethylhexyl thioglycolate (5 mol%) and 2.6-lutidine (10 mol%) in CH$_2$Cl$_2$ ([Monomer] = 1 M) at r.t
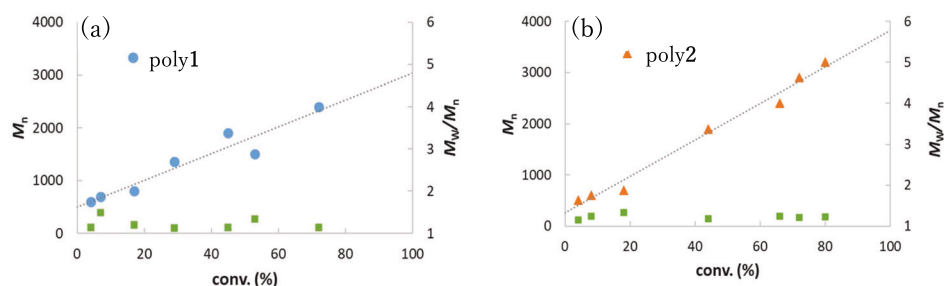
UV. UV-detected GPC profile is monomodal, however, with two shoulders in the higher and lower molecular weight regions; the former is probably due to disulfide-forming coupling at the polymer terminals, and the latter is ascribable to the cyclic polymer slightly involved in the starting polymer.

Anionic polymerization in 2,6-lutidine as the solvent

The polymerization of monomer **3** using a catalytic amount of 2,6-lutidine (Entry 10, Table 2) was so slow that 2,6-lutidine was used as the polymerization solvent. As shown in Table 3, the polymerization was accelerated; however, a decrease in the amount of initiator did not increase the molecular weight of the polymer. This finding prompted us to investigate whether the polymerization can occur even in the absence of the thiol initiator. As a result, monomer **1** was found to undergo polymerization in 2,6-lutidine without a thiol initiator (Entries 1–3, Table 4); however, multimodal GPC profiles were obtained (Fig. 7). The MALDI-

TOF-MS spectrum of the polymerization mixture revealed that a cyclic polymer was exclusively produced (Fig. 8). The polymerization is reasonably initiated via nucleophilic attack of 2,6-lutidine on the thioester carbonyl group of **1**, and the generated zwitterion propagates at the thiolate anion site (Scheme 3).

The backbiting reaction to the initiating end cation produces a high-molecular-weight cyclic polymer (route A in Scheme 3), and that to the polymer main chain results in the formation of smaller rings (route B in Scheme 3). It is reasonable that a lower monomer concentration decreases the molecular weight of the product polymer (Entries 1, 2, and 3, Table 4) by increasing the relative rate of the backbiting reaction (first-order for the concentration) in comparison with the propagation rate (second-order for the concentration). Figure 7 shows that the molecular weights of the product polymers decreased with increasing reaction time. The cyclic polymers undergo nucleophilic ring-opening by a large amount of 2,6-lutidine at the thioester carbonyl group, and the thiolate anion site of the generated

Fig. 2 ^{1}H NMR spectrum (CDCl$_3$) of the reaction mixture after 3 days of Entry 1 (Table 2)

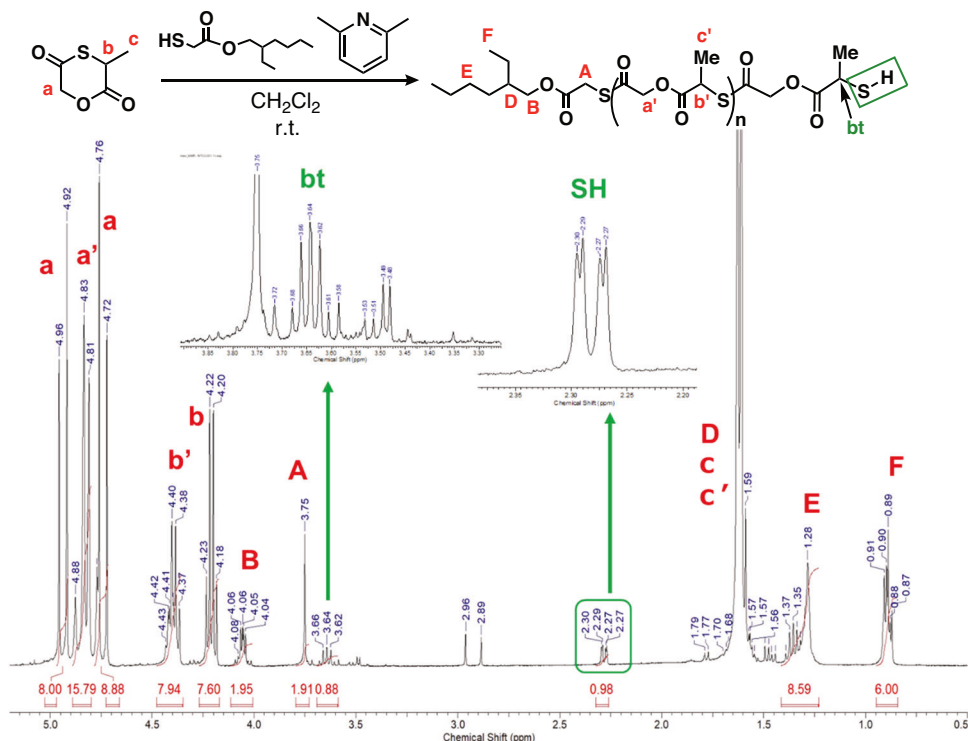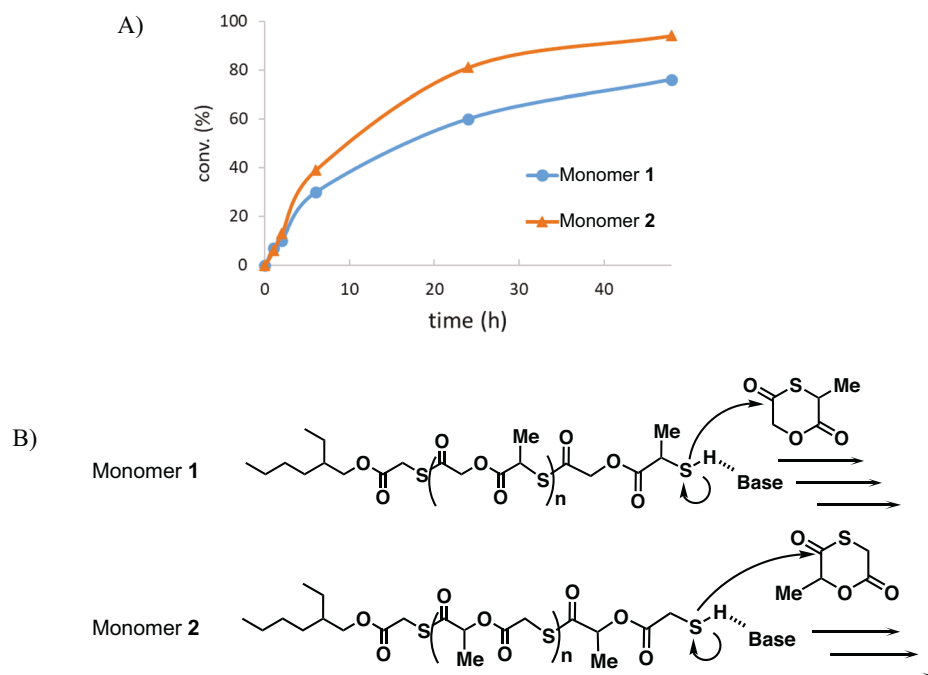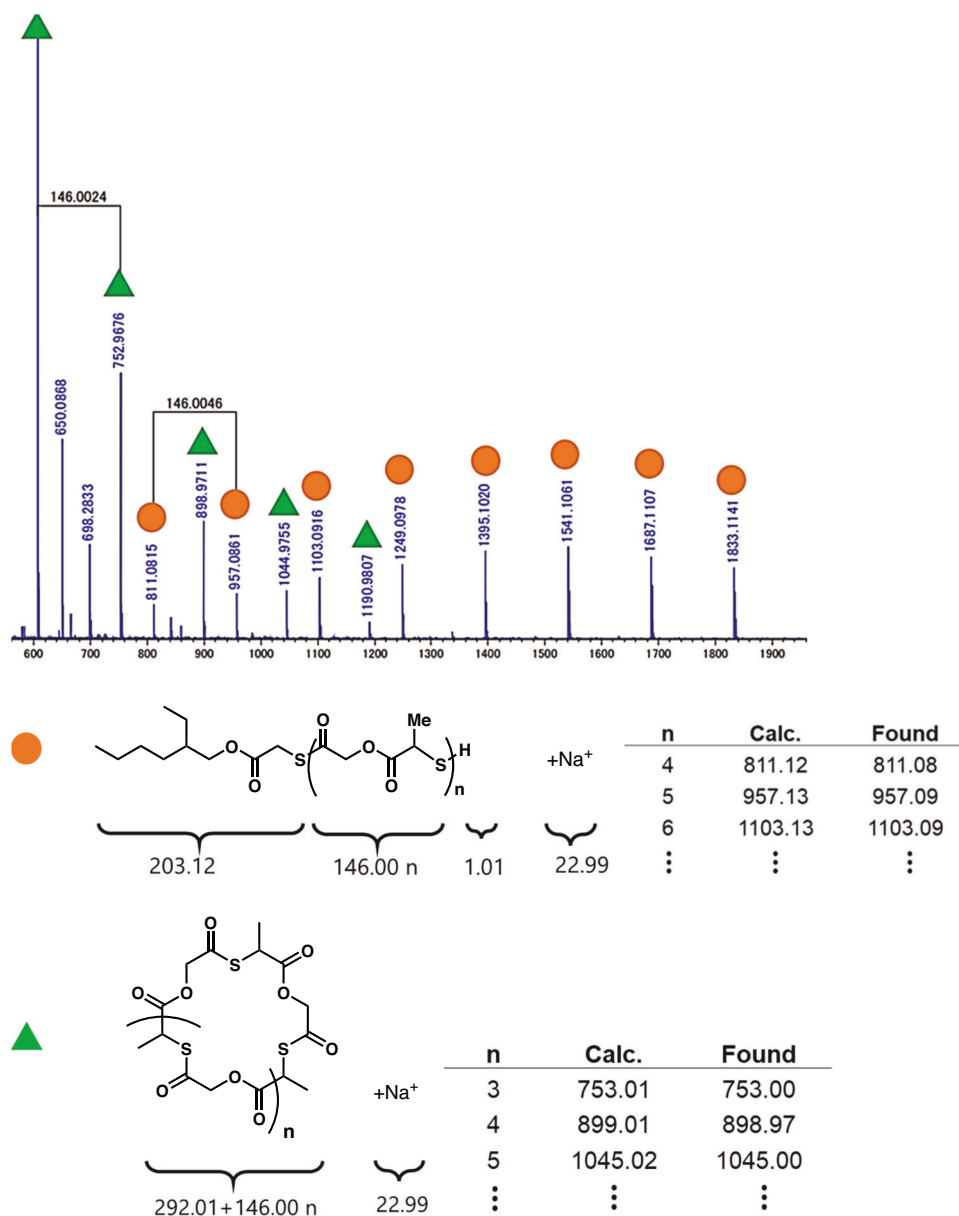**Fig. 3 A** Time-conversion curves of the polymerizations of monomers **1** and **2** in the presence of 2-ethylhexyl thioglycolate (5 mol%) and 2,6-lutidine (10 mol%) in CH$_2$Cl$_2$ ([Monomer] = 1 M) at r.t. **B** Propagations in the polymerizations of monomers **1** and **2**

zwitterion undergoes backbiting to form smaller rings. Monomers **2** and **3** are also polymerizable without the thiol initiator, producing cyclic polymers, as suggested by the MALDI-TOF-MS spectra (Figs. S27 and S28). Since monomer **2** is insoluble in 2,6-lutidine, a mixed solvent of 2,6-lutidine and CH$_2$Cl$_2$ (1/1 v/v) was used. The relative polymerization rates of the three monomers are **2** > **1** > **3** (Entries 4–6, Table 4), which are in the same order as those in the presence of the thiol initiator in CH$_2$Cl$_2$ (Table 1, vide supra). Monomer **2** gave a higher molecular weight polymer because of the larger ratio of the propagation rate to the backbiting reaction rate. The polymer from **3** showed an

Fig. 4 MALDI-TOF-MS spectrum of the polymerization mixture of monomer **1** (Entry 2, Table 2)

n	Calc.	Found
4	811.12	811.08
5	957.13	957.09
6	1103.13	1103.09
⋮	⋮	⋮

n	Calc.	Found
3	753.01	753.00
4	899.01	898.97
5	1045.02	1045.00
⋮	⋮	⋮

unimodal GPC profile in the high-molecular weight region; this is probably due to steric hindrance, which favors the backbiting reaction to the cationic initiation terminal instead of to the polymer mid-chain.

As mentioned above, the direct attack of a base on the monomer hinders the control of the polymerization. Thus, a nonnucleophilic base, i.e., 2,6-di-*tert*-butylpyridine (DBP), was examined as the catalyst. As expected, no polymerizations occurred without a thiol initiator in DBP or DBP/CH$_2$Cl$_2$ (1:1) as the solvent for the three monomers. The addition of the thiol initiator induced polymerization, however, which was very slow at low initiator concentrations (Table S1). The steric bulkiness of the two tert-butyl groups of DPB hinders the activation of the thiol at the

propagating end. In addition, a backbiting reaction to the polymer mid-chain occurred, as suggested by the ESI-MS spectra (Fig. S29).

Cationic polymerization

The combination of PhCH$_2$OH as an initiator with CF$_3$SO$_3$H as an acid catalyst was examined for the cationic polymerization of the three monomers since it is an efficient system for the controlled polymerization of lactide via an activated monomer mechanism [16]. Monomers **1**, **2**, and **3** were found to undergo polymerization (Table 5). Decreasing the initiator amount increased the molecular weights of the product polymers with decreasing polymerization rates.

Fig. 5 Postpolymerization of monomers **1** and **2** in the presence of 2-ethylhexyl thioglycolate (6 mol%) and 2.6-lutidine (10 mol%)
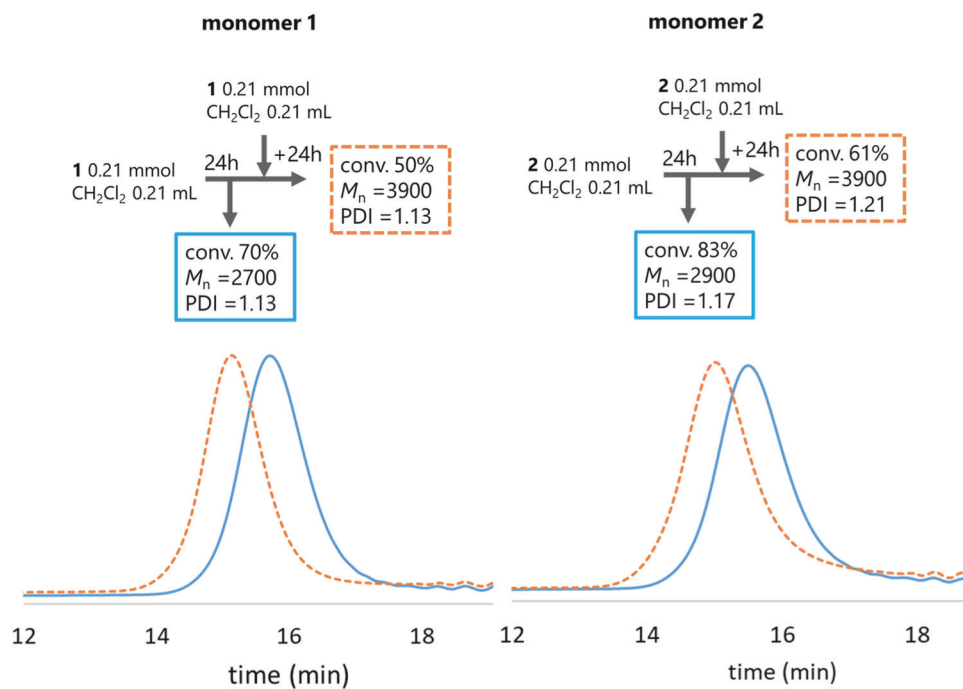
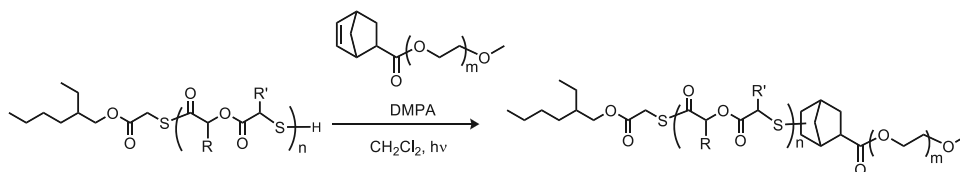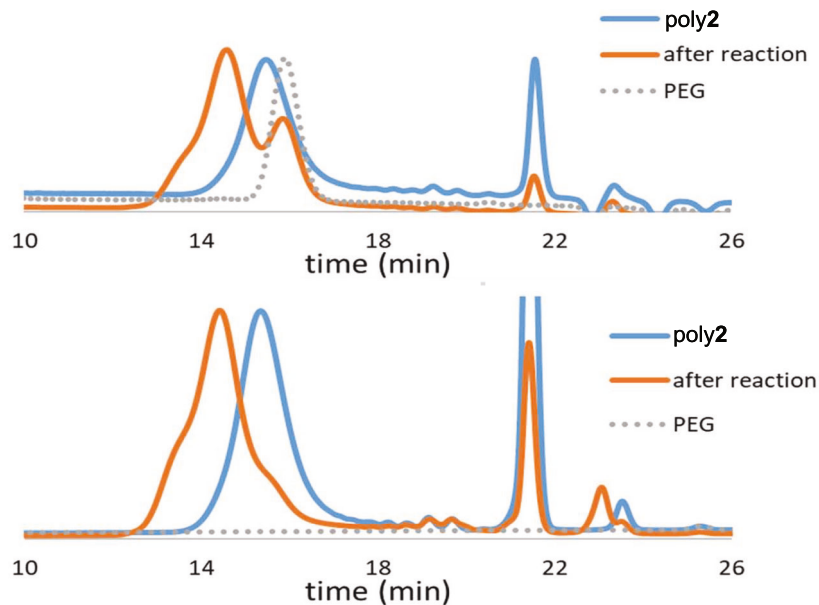**Scheme 2** Thiol-ene reaction to produce the block copolymer

Fig. 6 GPC profiles of the thiol-ene reaction mixture from poly**2**, detected by RI (upper) and UV (lower)

The ^{1}H NMR spectrum (Fig. S30) of the Et$_2$O-insoluble polymer from **1** showed a signal (5.17 ppm) due to the methylene protons of the benzyl ester group, supporting the initiation of the reaction. The MALDI-TOF-MS spectrum

(Fig. S31) revealed that PhCH$_2$OH was incorporated into the polymer terminals, but other unidentified peak series were observed. The polymerization mixtures from **2** and **3** showed no ^{1}H NMR signals due to the benzyl ester group

and provided no support according to their mass spectra (Figs. S32–S35).

The equimolar reactions between the monomers and PhCH$_2$OH in the presence of the CF$_3$SO$_3$H catalyst (5 mol%) were performed to obtain information about the chemoselectivity of the ring-opening reactions. The ^{1}H NMR spectrum of the reaction mixture from **1** (Fig. S36) showed signals due to the thiol and methine protons of the -CH(Me)SH structure, which is formed by ring opening at the thioester site. However, the relative integral intensities of these signals (0.24 and 0.27 for 1H and 1H, respectively) are smaller than the theoretical values based on the signal intensities of the phenyl and benzylic protons (5.00 and 1.94 for 5H and 2H, respectively) of the benzyl ester group. This finding suggests that ring opening occurs not only at the thioester site but also at the

oxoester site. The latter reaction produces the -CH$_2$OH structure, whose methylene protons labeled as i are detected as overlapping signals, whose relative integral intensity is 1.82 for 3H in the ^{1}H NMR spectrum (Fig. S36). Thus, these relative signal intensities allow the selectivity ratio of the ring-opening site to be evaluated as thioester/oxoester = 24/76 ~ 39/61. The stoichiometric reactions of monomers **2** and **3** with PhCH$_2$OH were also investigated by ^{1}H NMR spectroscopy (Figs. S37 and S38), which indicated that the oxoester ester was mainly cleaved; however, many small signals attributed to side reactions were observed.

The chemoselectivity of ring cleavage is affected by the basicity of the carbonyl oxygen, which is protonated, and by steric hindrance around the carbonyl carbon. The latter factor can be excluded for the reaction of monomer **3**, which has α-methyl groups at each of the 3- and 6-positions of the ring. Accordingly, the above findings suggest that the oxoester has more basic carbonyl oxygen than does the thioester. The 6-methyl group of monomer **2** exerts steric hindrance on the thioester carbonyl, consequently maintaining the ring-opening at the oxoester site, whereas the 3-methyl group of monomer **1** disfavors the reaction at the oxoester. This finding is consistent with the above-mentioned experimental results. However, these chemoselective ring-opening reactions cannot be directly applied to ROP. As mentioned above, the benzyl ester group was not detected by ^{1}H NMR or mass spectrometry for the polymerization mixtures of monomers **2** and **3**. In the additional

Table 3 Anionic polymerization of monomer **3** in 2,6-lutidine as the solvent at r.t in the presence of 2-ethylhexyl thioglycolate as the initiator

Entry	Init. (mol%)	Time (day)	Conv.[a] (%)	M_n[b]	PDI[b]
1	5	1	83	3800	1.76
2	1.5	1	66	3100	1.76
		3	71	3300	1.92

[**3**] = 1 M

[a]Determined by ^{1}H NMR spectroscopy

[b]GPC (THF, PSt std.)

Table 4 Anionic polymerization of monomers **1**, **2**, and **3** in 2,6-lutidine as the solvent at r.t. without a thiol initiator

Entry	Solvent	Monomer[a]	Time (day)	Conv.[b] (%)	M_p[c]	M_n[d]	PDI[d]
1	2,6-Lutidine	**1** (1 M)	1	78	43,000/1800		
			4	93	47,500/1600		
2	2,6-Lutidine	**1** (0.5 M)	1	41	32,500/1500		
			7	90	24,000/800		
			13	91	700		
3	2,6-Lutidine	**1** (0.3 M)	1	32	15,500/1800		
			4	78	15,000/1300		
			15	92	700		
4	2,6-Lutidine:CH$_2$Cl$_2$ = 1:1	**1** (0.5 M)	0.25	12	28,000	18,600	1.26
			1	40	24,000/1800		
			4	89	24,000/1400		
5	2,6-Lutidine:CH$_2$Cl$_2$ = 1:1	**2** (0.5 M)	1	58	69,800	39,100	1.81
			4	88	77,000/3500		
6	2,6-Lutidine	**3** (1 M)	1	21	31,300	19,500	1.38
			4	52	45,200	25,300	1.79

[a]Monomer concentration in parentheses

[b]Determined by ^{1}H NMR spectroscopy

[c]Molecular weight at the peak tops of the GPC (THF, PSt std.) profile of the reaction mixture

[d]GPC (THF, PSt std.) profile of the reaction mixture

Fig. 7 GPC profiles of the polymerization mixtures of monomer **1** in 2,6-litidine without a thiol initiator. [**1**] = 0.5 M (left), and 0.3 M (right)
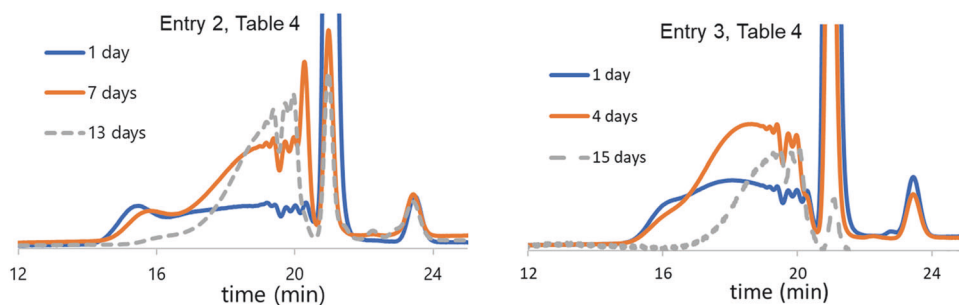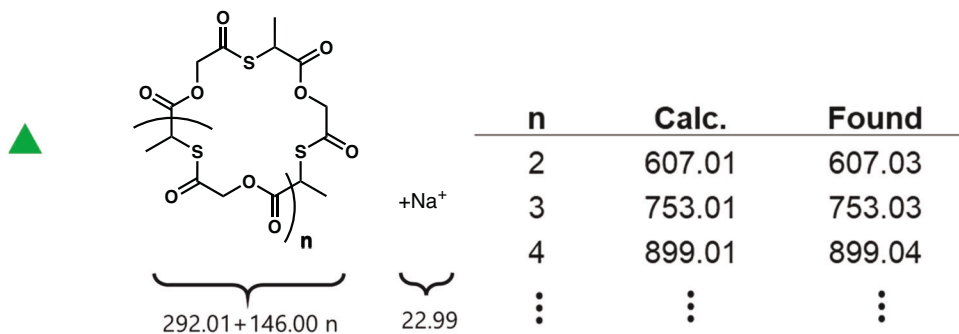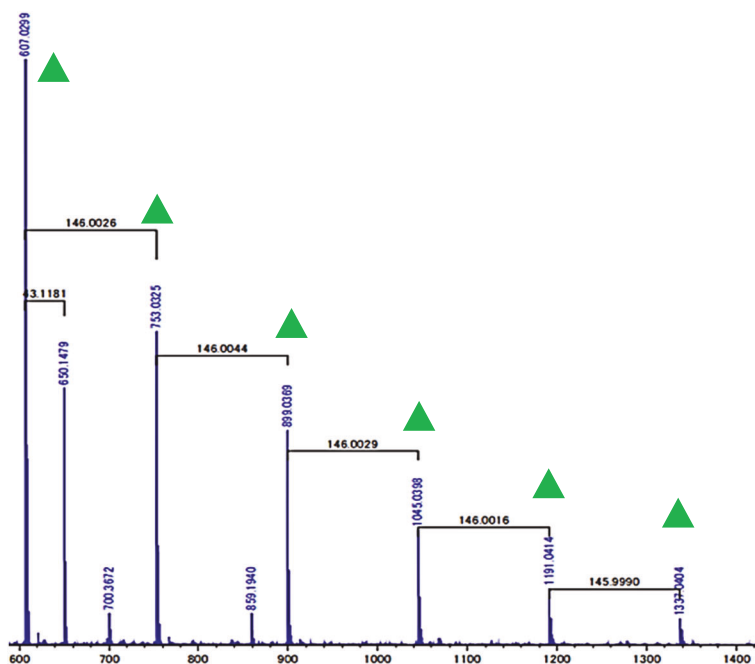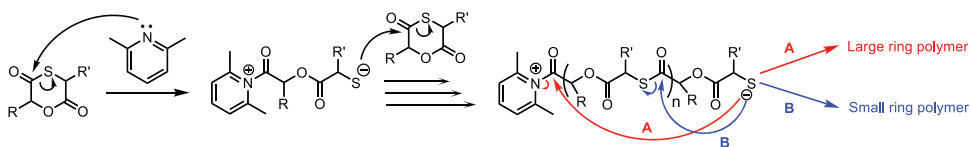

Fig. 8 MALDI-TOF-MS spectrum of the polymerization mixture (after 1 day) of monomer **1** in 2,6-lutidine without a thiol initiator (Entry 1, Table 4)

n	Calc.	Found
2	607.01	607.03
3	753.01	753.03
4	899.01	899.04
⋮	⋮	⋮

292.01+146.00 n   22.99

Scheme 3 Polymerization initiated with 2,6-litidine and the formation of cyclic polymers

experiment, when the amount of CF_3SO_3H was increased to 10 mol%, the polymer from monomer **1** also showed no benzyl ester group in the ^1H NMR spectrum. These inconsistencies are probably due to the low concentration of benzyl alcohol in the polymerization system, leading to ROP via the cationic chain-end mechanism instead of the activated monomer mechanism. To prevent side reactions and achieve a controllable ROP, CH_3CN, a more polar

Table 5 Cationic polymerization of monomers **1, 2,** and **3** in CH_2Cl_2 at r.t. using $PhCH_2OH$ as the initiator and CF_3SO_3H as the catalyst

Entry	Monomer[a]	$PhCH_2OH$ (mol%)	CF_3SO_3H (mol%)	Time (day)	Conv.[b] (%)	M_n[c]	PDI[c]
1	**1**	5	5	1	62		
				7	81	1500	1.72
2	**1**	1	5	6	65	3500	2.06
3	**2**	5	5	1	93	2500	1.54
4	**2**	2	5	1	91	3200	1.49
5	**3**	5	5	1	19	1500	1.38
				4	44	2400	1.53
6	**3**	2	5	1	15	1900	1.40
				4	39	2300	1.72

[a] [Monomer] = 1 M

[b] Determined by ^1H NMR spectroscopy

[c] GPC (THF, PSt std.)

solvent, and $(CF_3SO_2)_2NH$, a less acidic catalyst [17], were tested. Consequently, CH_3CN with CF_3SO_3H (5 mol %) accelerated the reaction but promoted frequent side reactions, producing an oligomer. $(CF_3SO_2)_2NH$ (10 mol %) also produced an oligomer in CH_2Cl_2 and no reaction in CH_3CN.

Thermal properties of the polymers obtained by the anionic polymerization

Since the T_g and T_{d10} (10%-weight-loss temperature) of low-molecular-weight polymers have some degree of dependence on the molecular weight, discussion about these parameters is limited herein (Table 6 and Figs. S39 and S40). However, it is obvious that the thioester group reduces the T_g compared with the oxoester. Thermal degradation is most likely initiated by the backbiting reaction of the thiol terminal; thus, poly**3** shows greater thermal stability than poly**1** and poly**2** because of steric hindrance due to the presence of two methyl groups. The backbiting reaction can lead to depolymerization of the monomer so that a more thermodynamically stable monomer with a smaller ring strain can be produced at a lower temperature. The lowest T_{d10} of poly(*rac*-thiolactide) is ascribed to the smallest ring strain of *rac*-thiolactide, as shown by the abovementioned DFT calculations.

Photodegradation of the polymers obtained by the anionic polymerization

Thioester absorbs UV at approximately 235 and 280 nm due to the π-π* and n-π* transitions, respectively. Our group previously demonstrated the photodegradation of poly(*rac*-thiolactide) [2]. Thus, polymers prepared from **1**, **2**, and **3** by the anionic polymerization were examined for UV degradation. The CH_2Cl_2 solutions of the polymers in

Table 6 Thermal properties of the polymers

|	M_n	PDI	T_g (°C)[a]	T_{d10} (°C)[b]
poly(*rac*-thiolactide)[c]	3860	1.5	−1 ~ 0	162
poly(*rac*-lactide)	–	–	35.5 ~ 65[d]	250[f]
poly**1**	3300	1.82	3.7	194
poly**2**	6100	1.15	16.2	209
poly**3**	3400	1.56	1.4	249

[a] Measured by DSC

[b] Temperature of 10%-weight loss measured by TG-DTA

[c] Ref. [2]

[d] SciFinder[n®]

[f] Ref. [18]

the quartz tubes were irradiated for 3 hr with a low-pressure Hg lamp, which has an emission band of 254 nm. The resultant polymers showed shifts in their GPC profiles to the lower molecular weight region (Fig. 9; S41 and S42). There was no large difference in the degradability among the three polymers. In contrast, poly(*rac*-lactide) showed little photodegradation under the same conditions (Fig. 9) since oxoester has almost no absorption at 254 nm.

Conclusion

Monomers **1** and **2**, which are cyclic cross-dimers composed of oxoester-thioester units from glycolic and thiolactic acids and from lactic and thioglycolic acids, respectively, underwent anionic ROP in a controlled manner to some extent by combining the thiol as the initiator with 2,6-lutidine as the catalyst in CH_2Cl_2 ant r.t. However, small amounts of cyclic polymers were involved. Monomer **3**, which is a cyclic cross-dimer from lactic and thiolactic

Fig. 9 GPC profiles of poly**3** (upper) and poly(*rac*-lactide) (lower) before and after UV irradiation in CH$_2$Cl$_2$ ([C(=O)S] = 68.2 mM and [C(=O)O] = 139 mM) for 3 h
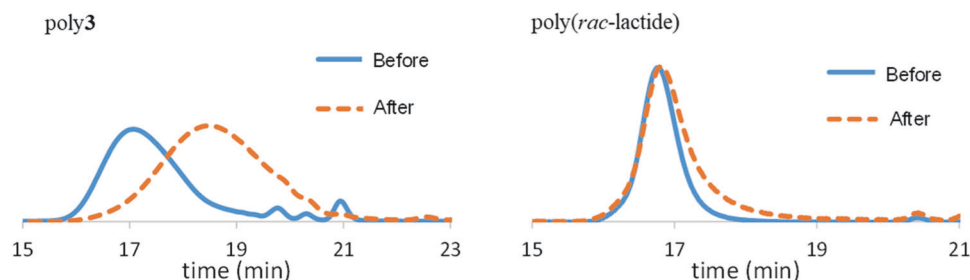
acids, requires 2,6-lutidine as the solvent for ROP. The absence of the thiol initiator in 2,6-lutidine exclusively produced macrocyclic polymers by backbiting reactions. In these polymerizations, the ring-opening occurred selectively at the thioester site, producing a polymer consisting of alternating oxoester-thioester units. The polymerization rates increased in the order of **3** < **1** < **2**, which was consistent with the increasing ring strain order evaluated by DFT calculations. The thioester unit caused the polymers to exhibit a lower T_g with greater thermal and photo degradability. The cationic ROPs of three monomers, **1**, **2**, and **3**, occurred in the presence of benzyl alcohol as the initiator with CF$_3$SO$_3$H as the catalyst in CH$_2$Cl$_2$ at r.t., but the selectivity of the ring-opening site was low, and frequent side reactions occurred to produce low-molecular-weight polymers.

Compliance with ethical standards

Conflict of interest The authors declare no competing interests.

Publisher's note Springer Nature remains neutral with regard to jurisdictional claims in published maps and institutional affiliations.

References

1. Suzuki M, Makimura K, Matsuoka S. Thiol-mediated controlled ring-opening polymerization of cysteine derived β-thiolactone and unique features of product polythioester. Biomacromolecules. 2016;17:1135–41.
2. Suzuki M, Watanabe A, Kawai R, Sato R, Matsuoka S, Kawauchi S. Ring-opening polymerization of thiolactide by using thiol-amine combination. Polymer 2021;215:123386. Corrigendum. 2022;242:124617
3. Suzuki M, Kaneko T, Ishikawa Y, Matsuoka S. Anionic polymerization of acrylic thioester by using organic base. Polym Chem. 2020;11:1145–50.
4. Wang C, Mavila S, Worrell BT, Xi W, Goldman TM, Bowman CN. Productive exchange of thiols and thioesters to form dynamic polythioester-based polymers. ACS Macro Lett. 2018;7:1312–6.
5. Aksakal S, Aksakal R, Becer CR. Thioester functional polymers. Polym Chem. 2018;9:4507–16.
6. Worrell BT, Mavila S, Wang C, Kontour TM, Lim C-H, McBride MK, et al. A User's guide to the thiol-thioester exchange in organic media: scope, limitations, and applications in material science. Polym Chem. 2018;9:4523–34.
7. Purohit VB, Pięta M, Pietrasik J, Plummer CM. Recent advances in the ring-opening polymerization of sulfur-containing monomers. Polym Chem. 2022;13:4858–78.
8. Illy N, Mongkhoun E. Thiolactone chemistry, a versatile platform for macromolecular engineering. Polym Chem. 2022;13:4592–614.
9. Li H, Guillaume SM, Carpentier J-F. Polythioesters prepared by ring-opening polymerization of cyclic thioesters and related monomers. Chem Asian J. 2022;17:e202200641.
10. Narmon AS, van Slagmaat CAMR, De Wildeman SMA, Dusselier M. Sustainable polythioesters via thio(no)lactones: monomer synthesis, ring-opening polymerization, end-of-life considerations, and industrial perspectives. ChemSusChem. 2023;16:e202202276.
11. Wang Y, Li M, Chen J, Tao Y, Wang X. O-to-S substitution enables dovetailing conflicting cyclizability, polymerizability, and recyclability: dithiolactone vs. Dilactone. Angew Chem Int Ed. 2021;60:22547–53.
12. Wang Y, Zhu Y, Lv W, Wang X, Tao Y. Tough while recyclable plastics enabled by monothiodilactone monomers. J Am Chem Soc. 2023;145:1877–85.
13. Ura Y, Al-Sayah M, Montenegro J, Beierle JM, Leman LJ, Ghadiri MR. Dynamic polythioesters via ring-opening polymerization of 1,4-thiazine-2,5-diones. Org Biomol Chem. 2009;7:2878–84. and references therein.
14. Takojima K, Makino H, Saito T, Yamamoto T, Tajima K, Isono T, et al. An organocatalytic ring-opening polymerization approach to highly alternating copolymers of lactic acid and glycolic acid. Polym Chem. 2020;11:6365–73.
15. Lozhkin BA, Shlyakhtin V, Bagrov VV, Ivchenko PV, Nifant'ev IE. Effective stereoselective approach to substituted 1,4-dioxane-2,5-diones as prospective substrates for ring-opening polymerization. Mendeleev Commun. 2018;28:61–3.

16. Bourissou D, Martin-Vaca B, Dumitrescu A, Graullier M, Lacombe F. Controlled cationic polymerization of lactide. Macromolecules. 2005;38:9993–8.

17. Makiguchi K, Kikuchi S, Satoh T, Kakuchi T. Synthesis of block and end-functionalized polyesters by triflimide-catalyzed ring-opening polymerization of e-caprolactone, 1,5-dioxepan-2-one, and rac-lactide. J Polym Sci Polym Chem. 2013;51:2455–63.

18. Sivalingam G, Madras G. Thermal degradation of binary physical mixtures and copolymers of poly(ε-caprolactone), poly(D, L-lactide), poly(glycolide). Polym Degrad Stab. 2004;84:393–8.